

Pictures of Hyperbolic Dynamical Systems

Yves Coudene

Introduction

Computer-generated pictures of fractals and attractors are quite common on the internet. The *Mandelbrot set*, the *Lorentz attractor*, and the *Henon attractor* are amongst the most represented dynamical systems on the web. Pictures and computer experiments have proven to be quite useful for their study. In some cases, computer-assisted proofs of their “chaotic” behavior are the only proofs available.

These systems all fall into the category of systems exhibiting non-uniformly hyperbolic behavior. Their study is modelled on the theory of uniformly hyperbolic dynamical systems and tries to recover some of the most prominent features of the hyperbolic theory: invariant SRB measures, bernoullicity of these measures, distribution results concerning the repartition of typical orbits, etc.

The modern theory of uniformly hyperbolic systems goes back to the middle of the twentieth century, with the work of D. V. Anosov [An67] and S. Smale [Sm67]. It is now a well-established theory and gives a pretty complete description of the dynamics of smooth systems whose differential is uniformly contracting and dilating on two invariant complementary sub-bundles of the tangent space. The theory provides numerous examples of non-trivial attractors and gives a nice description of the dynamic on these attractors by the use of a symbolic model.

As strange as it may seem, there are almost no pictures of these uniformly hyperbolic attractors. There may be several reasons for that; the theory was built during the 1960s and 1970s; at that time, computers were not powerful enough to handle the computations. Also computer experiments are usually focused on systems of physical origin. These systems are often of the non-uniformly hyperbolic type.

Yves Coudene is professor of mathematics at IRMAR, Université Rennes 1, France. His email address is yves.coudene@univ-rennes1.fr.

We explain how to obtain pictures of three of the most famous hyperbolic surface diffeomorphisms, namely the *attractor derived from Anosov*, the *Plykin attractor*, and a *Smale horseshoe*, and how to build a paper-model of four entangled Wada lakes on the sphere. The transformations are built by perturbing a toral automorphism, following a recipe that can be found, for example, in the book of J. Palis and W. de Melo [PaDM82].

Attractors Derived from Anosov

The first example is due to S. Smale [Sm67]; it is obtained by perturbing an Anosov diffeomorphism. Hence it is called an *attractor derived from Anosov*. This attractor is defined on the two-dimensional torus \mathbf{T}^2 . The torus may be seen as a product of two circles $\mathbf{S}^1 \times \mathbf{S}^1$, or as the quotient of the plane \mathbf{R}^2 by the subgroup \mathbf{Z}^2 of points with integer coordinates: $\mathbf{T}^2 \simeq \mathbf{R}^2/\mathbf{Z}^2$.

Hyperbolic Automorphism of the Torus

We first need some properties of the matrix $A = \begin{pmatrix} 2 & 1 \\ 1 & 1 \end{pmatrix}$. Let us denote the golden mean by $\lambda = \frac{1+\sqrt{5}}{2} \simeq 1.618$. The matrix A admits two eigenvalues λ^2 and λ^{-2} ; the associated eigenvectors are $\mathbf{e}_u = \frac{1}{\sqrt{1+\lambda^2}} \begin{pmatrix} \lambda \\ 1 \end{pmatrix}$ and $\mathbf{e}_s = \frac{1}{\sqrt{1+\lambda^2}} \begin{pmatrix} -1 \\ \lambda \end{pmatrix}$, and the following relation holds:

$$\begin{pmatrix} 2 & 1 \\ 1 & 1 \end{pmatrix} = \frac{1}{\sqrt{1+\lambda^2}} \begin{pmatrix} \lambda & -1 \\ 1 & \lambda \end{pmatrix} \begin{pmatrix} \lambda^2 & 0 \\ 0 & \lambda^{-2} \end{pmatrix} \frac{1}{\sqrt{1+\lambda^2}} \begin{pmatrix} \lambda & 1 \\ -1 & \lambda \end{pmatrix}$$

The action of the matrix $\begin{pmatrix} 2 & 1 \\ 1 & 1 \end{pmatrix}$ on the plane gives an invertible transformation on the torus \mathbf{T}^2 , called a *hyperbolic toral automorphism*. This transformation is an Anosov diffeomorphism: there are two invariant uniformly contracting and dilating sub-bundles in the tangent space. The contracting one is directed by \mathbf{e}_u at each point, the dilating one by \mathbf{e}_s .

The following can be shown about the dynamics of the toral automorphism:

- the periodic points are dense;

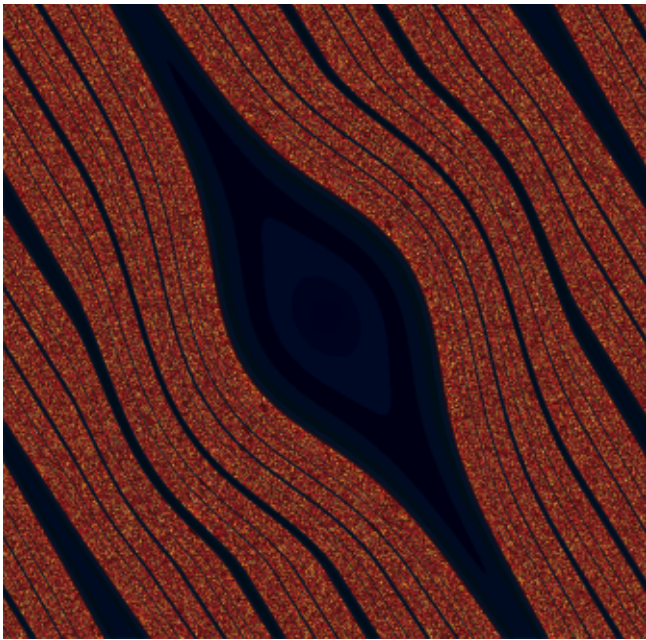


Figure 1.

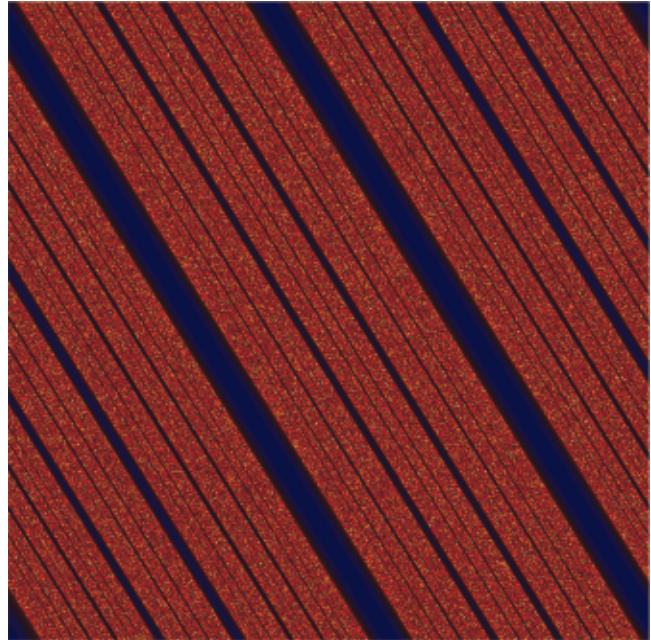


Figure 2.

Figure 2 (r.) is an enlargement of a small part of Figure 1 (l.), centered on the point $\begin{pmatrix} 0.5 \\ 0.5 \end{pmatrix}$. It reveals a structure of the type “Cantor times interval” in the complement of the basin of attraction.

- there exists a point whose orbit is dense;
- there are many ergodic invariant probability measures with full support.

These properties show that the dynamic of the transformation is indeed quite intricate. They can be obtained by the use of a symbolic model and are in fact shared by all transitive Anosov diffeomorphisms. The survey of J.C. Yoccoz [Yoc95] contains a nice presentation of these results.

The Perturbation

We now add a term to the diffeomorphism, so as to transform the fixed point $\begin{pmatrix} 0 \\ 0 \end{pmatrix}$ into an attracting fixed point.

$$f_1 : \begin{pmatrix} x \\ y \end{pmatrix} \mapsto \begin{pmatrix} 2 & 1 \\ 1 & 1 \end{pmatrix} \begin{pmatrix} x \\ y \end{pmatrix} + \frac{p_1}{1 + \lambda^2} k(x/a)k(y/a) \begin{pmatrix} \lambda^2 & \lambda \\ \lambda & 1 \end{pmatrix} \begin{pmatrix} x \\ y \end{pmatrix}$$

with $k(x) = (1 - x^2)^2 \mathbf{1}_{[-1,1]}(x)$ used as a C^1 “bump” function. The parameter a controls the extent of the perturbation, the parameter p_1 controls its amplitude. The additional term only modifies the dominant eigenvalue. The differential at the fixed point $\begin{pmatrix} 0 \\ 0 \end{pmatrix}$ is now conjugated to $\begin{pmatrix} \lambda^2 + p_1 & 0 \\ 0 & \lambda^{-2} \end{pmatrix}$.

Note that $\lambda_2 \simeq 2.618$; so if we choose $p_1 = -2.2$, the point $\begin{pmatrix} 0 \\ 0 \end{pmatrix}$ becomes an attracting fixed point. If the parameter a is less than 0.5, say $a = 0.4$, the periodic point $\begin{pmatrix} 0.5 \\ 0.5 \end{pmatrix}$ of A is again a hyperbolic periodic point for f_1 . Hence not all points are attracted by $\begin{pmatrix} 0 \\ 0 \end{pmatrix}$. So, we may expect to see an open set of points attracted to the point $\begin{pmatrix} 0 \\ 0 \end{pmatrix}$, whereas there is still an invariant compact set on which the dynamics retains some of the features of the

hyperbolic toral automorphism. This is indeed what happens for the chosen set of parameters. The basin of attraction of the point $\begin{pmatrix} 0 \\ 0 \end{pmatrix}$ is depicted in Figure 1.

Let us explain how it was obtained. For each pixel on the picture, we calculate the number of iterations needed to reach a small neighborhood of the attracting fixed point $\begin{pmatrix} 0 \\ 0 \end{pmatrix}$, say the disk $\{(x, y) \mid x^2 + y^2 < 0.0001\}$. The pixel is colored according to that number of iterations: points that take less than ten iterations to reach the small disk are colored in black. The intensity of the color

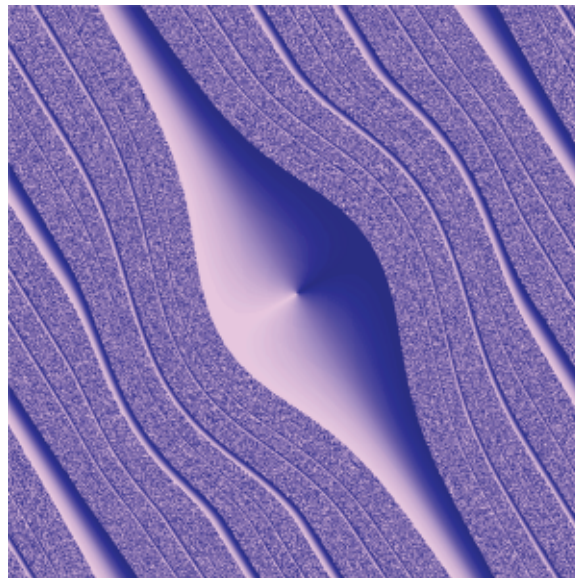


Figure 3.

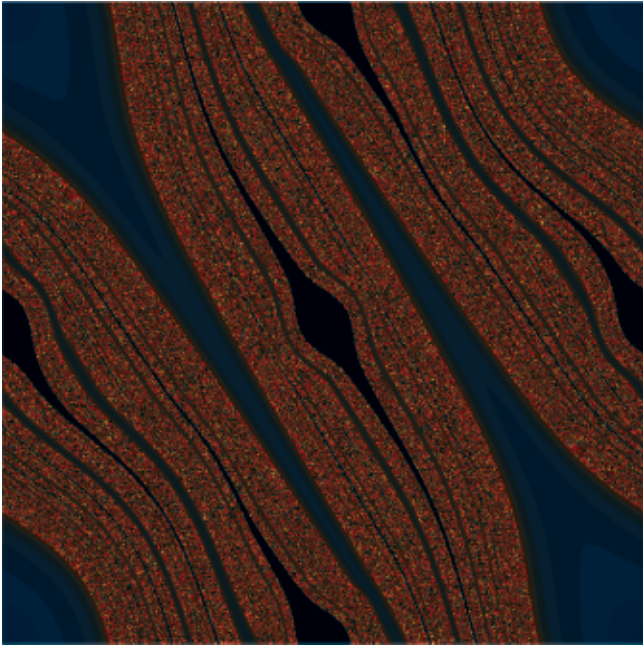


Figure 4.

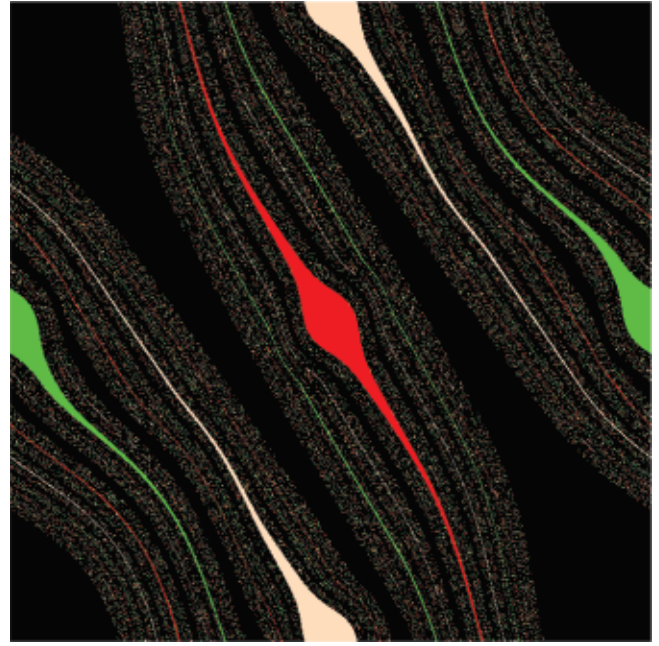


Figure 5.

then increases until thirty iterations are needed, in which case the pixel appears in red. Pixels in yellow need around seventy iterations. Points needing more than two hundred iterations should appear in bright white, although they are hard to spot on the picture. Of course, points needing more than ten iterations to reach the small disk around the attracting fixed point are very close to the boundary of the basin of attraction; thus the colored area on Figure 1 almost coincides with the complement of the basin.

Other algorithms can be used to get a glimpse at that basin of attraction. In Figure 3, we first color the small disk $\{(x, y) \mid x^2 + y^2 < 0.0001\}$ radially. Points in the direction of $-\mathbf{e}_u$ are colored in white; the color smoothly fades until it reaches dark blue, which is attained for points in the direction of \mathbf{e}_u . Each pixel is then colored according to the color of the first iterate which falls into the small disk.

We now consider the inverse of the transformation f_1 , instead of f_1 . The point $\begin{pmatrix} 0 \\ 0 \end{pmatrix}$ is a repelling fixed point for f_1^{-1} . The complement of its basin of repulsion is an attractor; it is called an *attractor derived from Anosov*. The bright part in Figure 1 forms a small neighborhood of that attractor, and it corresponds to the “noisy” part in Figure 3.

The noise reflects the fact that the dynamic on the attractor is “chaotic”: the set of periodic points is dense, there are points with dense orbits; in fact it retains all the prominent features of the dynamics of the toral automorphism.

The Plykin Attractor

The attractor derived from Anosov lives on the torus. One can ask if there are uniformly hyperbolic

attractors on the sphere. The first example of such a system was given by Plykin [Ply74]; it can be obtained from the attractor derived from Anosov by realizing the sphere as a quotient of the torus.

Second Deformation

We first make another deformation to the map f_1 , in order to obtain other attracting basins. The orbit of the point $\begin{pmatrix} 0.5 \\ 0.5 \end{pmatrix}$ is periodic of period three under the transformation f . Indeed we have:

$$\begin{aligned} f_1 \begin{pmatrix} 0.5 \\ 0.5 \end{pmatrix} &= \begin{pmatrix} 0.5 \\ 0 \end{pmatrix}, \\ f_1 \begin{pmatrix} 0.5 \\ 0 \end{pmatrix} &= \begin{pmatrix} 0 \\ 0.5 \end{pmatrix}, \\ f_1 \begin{pmatrix} 0 \\ 0.5 \end{pmatrix} &= \begin{pmatrix} 0.5 \\ 0.5 \end{pmatrix}. \end{aligned}$$

Let us denote the integer part of some real number x by $E(x)$. The following change of variables:

$$\begin{cases} x_2 = x - 0.5 E(2x + 0.5) \\ y_2 = y - 0.5 E(2y + 0.5) \end{cases}$$

sends the three periodic points to the center $\begin{pmatrix} 0 \\ 0 \end{pmatrix}$. In order to transform these points into attracting periodic points, we add another term to the map f_1 and consider the map $f_2 : \mathbb{T}^2 \rightarrow \mathbb{T}^2$ sending $\begin{pmatrix} x \\ y \end{pmatrix}$ to:

$$\begin{aligned} \begin{pmatrix} 2 & 1 \\ 1 & 1 \end{pmatrix} \begin{pmatrix} x \\ y \end{pmatrix} + \frac{p_1 k(\frac{x}{a})k(\frac{y}{a})}{1 + \lambda^2} \begin{pmatrix} \lambda^2 & \lambda \\ \lambda & 1 \end{pmatrix} \begin{pmatrix} x \\ y \end{pmatrix} \\ + \frac{p_2 k(\frac{x_2}{b})k(\frac{y_2}{b})}{1 + \lambda^2} \begin{pmatrix} \lambda^2 & \lambda \\ \lambda & 1 \end{pmatrix} \begin{pmatrix} x_2 \\ y_2 \end{pmatrix} \end{aligned}$$



Figure 6.

We take $a = 0.4$ and $b = 0.1$, so that the two perturbations do not interfere. The differential of f_2 at the three periodic points is conjugate to $\begin{pmatrix} \lambda^2 + p_2 & 0 \\ 0 & \lambda^{-2} \end{pmatrix}$. The periodic orbit of period three becomes attractive if, for example, $p_2 = -2.2$.

The result is depicted in Figure 4. That figure is centered on the periodic point $\begin{pmatrix} 0.5 \\ 0.5 \end{pmatrix}$. Its basin of attraction appears in black. The algorithm used for that picture is similar to the algorithm of Figure 1. The inverse of the third iterate of f_2 , f_2^{-3} admits four repelling fixed points; the complement of the basin of repulsion of these four points is an attractor, on which the dynamics enjoys properties similar to the hyperbolic automorphism of the torus. The four basins of repulsion are depicted in different colors in Figure 5.

From the Torus to the Sphere

We now consider the symmetry on the torus given by $(x, y) \mapsto (-x, -y)$. This symmetry has four fixed points, which are precisely the fixed point of f_2 and the three periodic points of period three. We may quotient the torus by this symmetry. The resulting space

is topologically a sphere; from the differential viewpoint, it is a sphere with four conical points. Such a space has a euclidean model, namely the tetrahedron. If we start from the hexagonal torus instead of the usual one, the resulting tetrahedron is regular.

The transformation f_2^{-1} commutes with the symmetry, so it defines a transformation of the tetrahedron, for which the four vertices are repelling fixed points. The *Plykin attractor* is obtained by smoothing the tetrahedron and the transformation f_2^{-1} in a neighborhood of the vertices. Note that if the smoothing is small enough, it takes place in the basins of repulsion of the repelling points and does not alter the attractor. So, for the purpose of representation, this smoothing is irrelevant. Figure 6 gives an explicit model for the tetrahedron, which can be cut and pasted to obtain a representation of the Plykin attractor.

Lakes of Wada

Finally, the sphere or the tetrahedron may be stereographically projected on the plane. The repelling

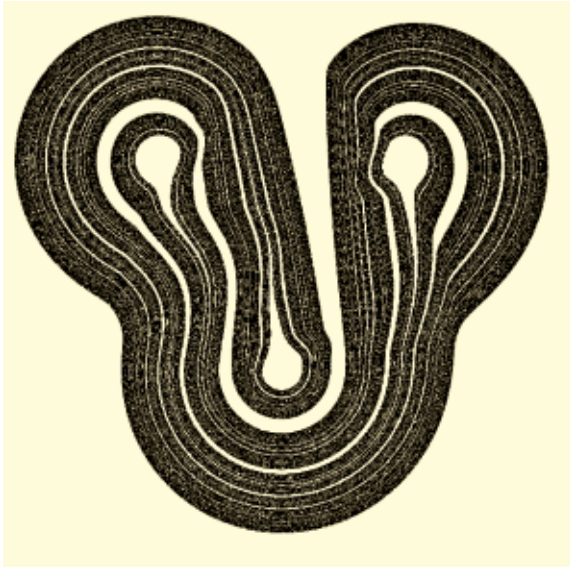


Figure 7.

fixed point $\begin{pmatrix} 0 \\ 0 \end{pmatrix}$ on the torus is sent to infinity by the projection. The map obtained from f_2^{-1} is a diffeomorphism of the plane, for which infinity is repelling; it admits moreover a period three repelling orbit, and the complement of the basins of repulsion is an attractor which is depicted in Figure 7.

Note that the basins of repulsion of the transformation form Lakes of Wada: each of the four basins is an immersed disk, and each of these disks has the same boundary, the attractor itself. In other words, any point on the attractor is accumulated by the four basins of repulsion. Such immersion of disks in the plane was first built by L. Brouwer, K. Yoneyama [Yon17]. The basins are depicted in different colors in Figure 8.

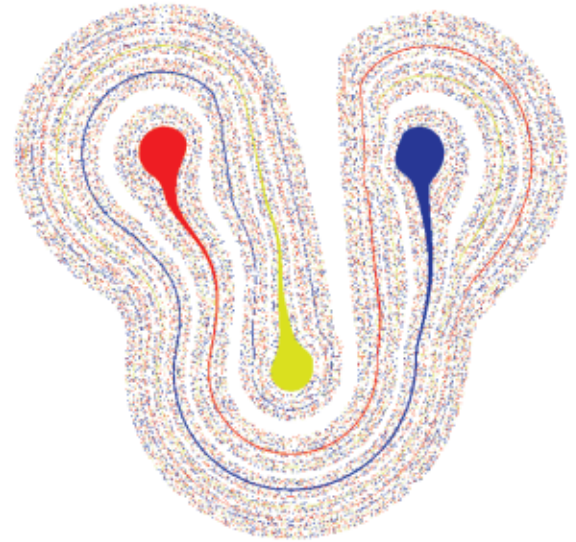


Figure 8.

The Smale Horseshoe

Third deformation

We come back to the transformation f_1 on the torus. What happens if the periodic orbit of period three of f_1 is deformed into a repelling periodic orbit instead of an attracting periodic orbit? Such a deformation can be achieved by adding a third term to the automorphism of the torus:

$$f_3 \begin{pmatrix} x \\ y \end{pmatrix} = f_2 \begin{pmatrix} x \\ y \end{pmatrix} + \frac{p_3}{1 + \lambda^2} k\left(\frac{x_2}{a}\right)k\left(\frac{y_2}{a}\right) \begin{pmatrix} x_2 \\ y_2 \end{pmatrix}$$

The parameter p_3 determines the amplitude of the perturbation. The eigenvalues of Df_3 at the periodic points of period three are equal to $\lambda^2 + p_2 + p_3$ and $\lambda^{-2} + p_3$. We take $p_2 = -2.2$, $p_3 = 0.7$.

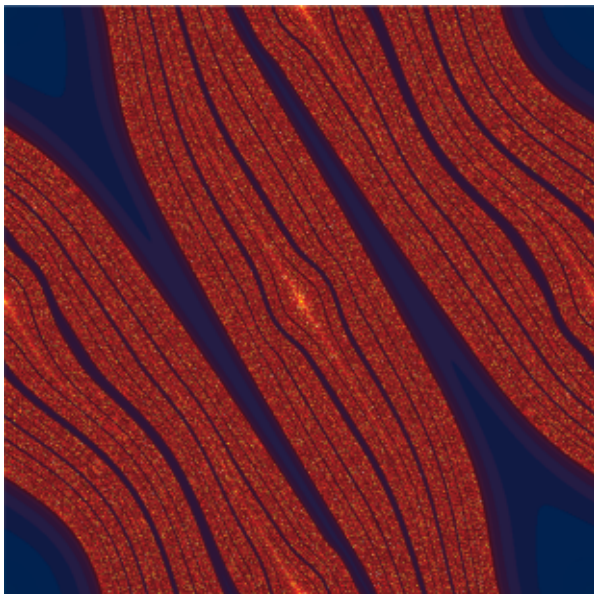


Figure 9.

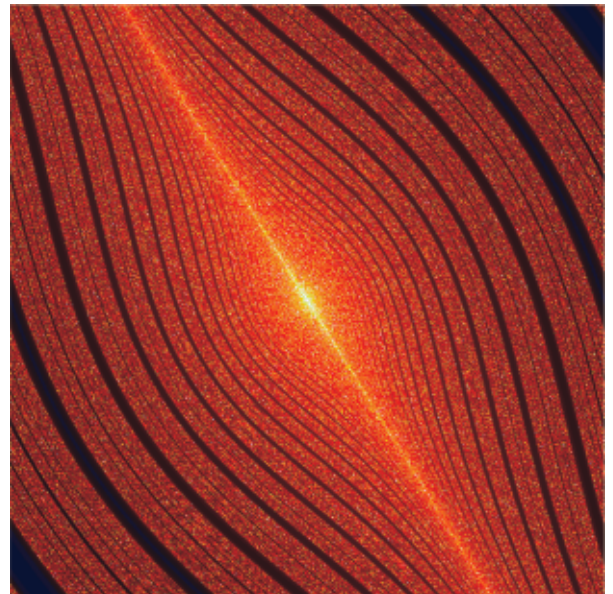


Figure 10.

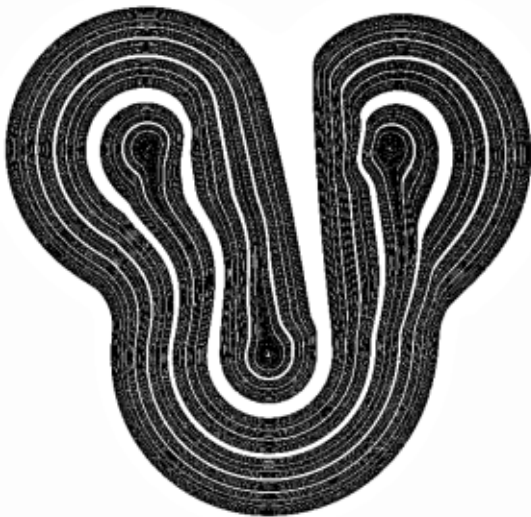


Figure 11.

The result is shown in Figure 9; the algorithm used is the same as in Figures 1 and 2. The figure is centered on the point $\begin{pmatrix} 0.5 \\ 0.5 \end{pmatrix}$. Note that colors around this point seem to be brighter, compared to Figure 1. Figure 10 shows an enlargement around $\begin{pmatrix} 0.5 \\ 0.5 \end{pmatrix}$ and should be compared with Figure 2. We can see how the basin of attraction of the point $\begin{pmatrix} 0.5 \\ 0.5 \end{pmatrix}$ (in black on the picture) is repelled by the point $\begin{pmatrix} 0.5 \\ 0.5 \end{pmatrix}$.

Horseshoes

The transformation f_3 on the torus induces a mapping on the sphere, which exhibits a “Smale horseshoe”. It possesses a repelling orbit of period three, and infinity is an attracting fixed point.

The compact set K depicted in Figure 11 ($p_4 = 0$) consists of the points which are not attracted by infinity. This set may be split into three invariant

subsets: the repelling orbit of period three; a Cantor set consisting of the closure of the recurrent points of f_3 (different from the three repelling points); and the set of points which are attracted by this Cantor set. The closure of the recurrent points is the set usually called the *horseshoe*.

Figure 12 is a colored version of Figure 11, whereas Figure 13 is an enlargement of Figure 12 around one of the three repelling points. The brighter the points, the longer it takes to reach infinity; hence the colored part forms a neighborhood of the set of points which do not go to infinity.

Acknowledgment

All pictures were generated using the free software FRACTINT [Fr].

References

- [An67] D. V. ANOSOV, Geodesic flows on closed riemannian manifolds with negative curvature, *Proc. Steklov Inst. Math.* **90** (1967).
- [Fr] The software FRACTINT can be downloaded from <http://www.fractint.org>.
- [Ply74] R. V. PLYKIN, Sources and sinks of A-diffeomorphisms of surfaces (Russian), *Mat. Sb. (N.S.)* **94**(136) (1974), 243–264, 336.
- [PaDM82] J. PALIS and W. DE MELO, *Geometric theory of dynamical systems. An introduction*, Translated from the Portuguese by A. K. Manning, Springer-Verlag, New York-Berlin, 1982.
- [Sm67] S. SMALE, Differentiable dynamical systems, *Bull. AMS* **73** (1967), 747–817.
- [Yoc95] J. C. YOCCOZ, *Introduction to hyperbolic dynamics. Real and complex dynamical systems* (Hillerød, 1993), 265–291, NATO Adv. Sci. Inst. Ser. C Math. Phys. Sci., 464, Kluwer Acad. Publ., Dordrecht, 1995.
- [Yon17] K. YONEYAMA, Theory of continuous set of points, *Tohoku Math. J.* 11–12, 43 (1917).

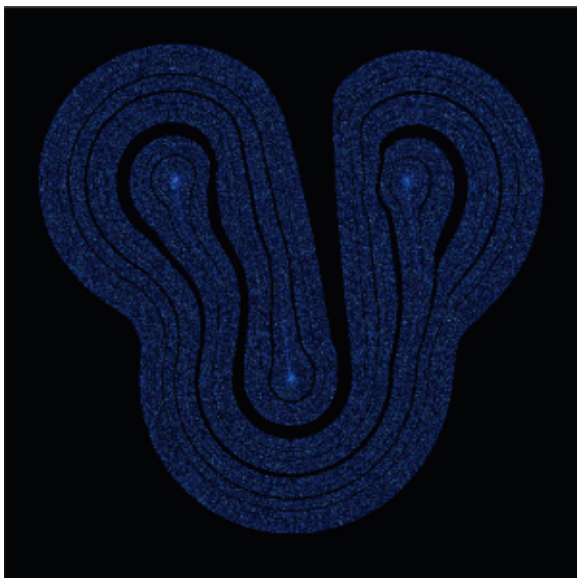


Figure 12.

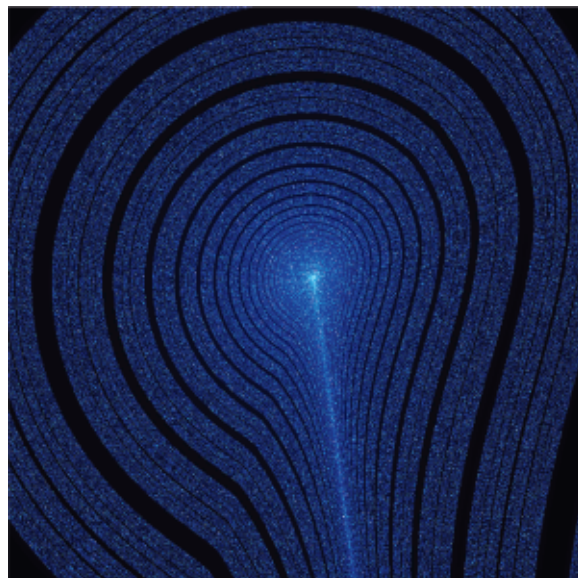


Figure 13.